JOURNAL OF BIOMEDICAL OPTICS 1(1), 110–116 (JANUARY 1996)

OPTICAL PROPERTIES OF SCATTERING AND ABSORBING MATERIALS USED IN THE DEVELOPMENT OF OPTICAL PHANTOMS AT 1064 NM

David D. Royston,[†] Regan S. Poston,[‡] and Scott A. Prahl*

[†]Food and Drug Administration, 5600 Fishers Lane, HFZ-134, Rockville, Maryland 20857;
[‡]University of Pennsylvania, Department of Bioengineering, Philadelphia, Pennsylvania 19104-6392;
*St. Vincent Hospital and Medical Center, Oregon Medical Laser Center, 9205 Southwest Barnes Road, Portland, Oregon 97225

(Paper JBO-025 received July 26, 1995; revised manuscript received Nov. 7, 1995; accepted for publication Nov. 21, 1995)

ABSTRACT

Optical phantoms have been developed to simulate the distribution of visible light in tissue. These phantoms can then be used to evaluate the performance of optical fiber delivery and/or radiometric detecting systems. This paper describes the development of an optical phantom for the neodymiun/yttrium-aluminum-garnet (Nd:YAG) laser wavelength of 1064 nm and the absorption coefficient, scattering coefficient, and anisotropy of the media used in its development.

Key Words intralipid; phantoms; scattering coefficient; anisotropy.

1 INTRODUCTION

Optical phantoms have been developed to simulate the distribution of light in tissue.[1–3] These phantoms have been primarily designed in the red (630 nm) portion of the spectrum for use relevant to photodynamic therapy. Other phantoms have been designed for determining fluorescence quantum yields in the wavelength band extending from 300 to 650 nm. The phantoms consist of a scattering medium, an absorbing medium, a diluent, and in some cases fluorophores. Some common scattering media are Intralipid, Nutralipid, or Liposyn. The mention of commercial products or their use in connection with material reported here is not to be construed as either an actual or implied endorsement of such products by the U.S. Food and Drug Administration. These intravenously administered nutrients are fat emulsions that contain soybean oil, egg phospholipids, and glycerol. In addition to these fat emulsions, polystyrene microspheres have been used. These microspheres exhibit low fluorescence, and some of their optical properties can be calculated from Mie theory.[4] Absorbing media include some biological stains, such as trypan blue, Evans blue, and indocyanine green, as well as India ink. The diluent is usually deionized water although isotonic phosphate-buffered saline has been used. The optical properties of Intralipid[5] and India ink[6] have been previously studied at visible wavelengths. We have been interested in developing an optical phantom suitable for applications in the largely unexamined near-infrared range, particularly 1064 nm, the primary neodymium/yttrium-aluminum-garnet (Nd:YAG) laser wavelength.

An optical phantom is developed by mixing the correct proportions of the scattering and absorbing media in the diluent, so that the resulting suspension has the desired intrinsic optical properties of the simulated tissue. These intrinsic optical properties include the absorption coefficient (μ_a), the scattering coefficient (μ_s), and the anisotropy factor (g). For soft tissues, typical optical properties are μ_a =0.5 to 5.0 cm^{-1}, μ_s=100 cm^{-1}, and g=0.9 for near-infrared wavelengths.[7]

The Nd:YAG laser operating at the 1064-nm wavelength has been used clinically for some time.[8] One major physical advantage of this wavelength is that it can be delivered to target tissue through an optical fiber. This allows the laser light to be delivered to any surgical site that can be viewed with an endoscope. The absorption of visible and near-infrared radiation is primarily due to the presence of chromophores such as hemoglobin, flavins, cytochromes, and carotenoids. However, there is no known biologic chromophore that preferentially absorbs the 1064-nm wavelength of the Nd:YAG laser. Since this wavelength penetrates tissue more easily than visible wavelengths, it can produce excellent hemostasis. When it is used with either sapphire or sculpted silica scalpels, it can also be used for he-

Address all correspondence to David D. Royston. E-mail: dave@eob.cdrh.fda.gov

mostatic tissue dissection. Current clinical and laboratory research is focused upon using the 1064-nm laser wavelength to treat specific diseases such as benign prostatic hyperplasia[9] and cancer.[10–13]

The optical properties of a phantom need not be identical to those of the tissue, but they may be related by having the same tissue diffusion coefficient, D ($D = \mu_a / \mu_{\text{eff}}^2$ where μ_{eff}^2 is the effective attenuation coefficient, and $\mu_{\text{eff}}^2 = 3\mu_a[\mu_a + \mu_s(1 - g)]$). This allows the construction of phantoms that scatter and absorb light in the same manner as tissue, but over larger volumes.[14] Detecting fibers may then be conveniently placed in the phantom to record fluence levels. The ideal phantom combines a nonabsorbing scattering medium and a nonscattering absorbing medium. In practice, molecular absorbers can be found that contribute little or no scattering in the UV and visible wavelength range. However, India ink, the absorption medium used in some phantoms, is a water-insoluble pigment and has been shown to produce significant scattering with visible light.[6] Conversely, some scattering media, e.g., Intralipid suspensions, have been shown to have some (<0.01 cm^{-1}/%) absorption for visible wavelengths.[5,15]

In developing tissue optical phantoms for use at 1064 nm, we selected India ink as the primary absorber. It is readily available and has been characterized in phantoms used with other optical wavelengths. In addition, there does not appear to be a water-soluble, nontoxic molecular absorber for this wavelength. Our chosen scattering medium, Intralipid, has been employed in other phantom investigations, but has not been completely characterized at 1064 nm. Its ingredients are controlled and uniform, and it appears to have a long shelf life (for nonmedical purposes). It is also easy to prepare accurate dilutions that remain in suspension for hours at a time. This contrasts with polystyrene spheres that, depending upon diameter, may not remain in suspension without repeated agitation and require additional transmission measurements and Mie calculations in order to prepare accurate concentrations. However, for those phantoms that require an independent means of estimating their optical properties, polystyrene spheres with diameters less than 1 micron may be the appropriate choice.

Thus, a study was undertaken to determine the optical properties (μ_a, μ_s, g) of each medium and construct two tissue phantoms with predicted optical properties. Finally, the measured optical properties of the phantoms were compared with the predicted ones.

2 METHODS AND MATERIALS

Diffuse reflectance and transmission measurements of varying concentrations of either India ink (Pelikan, Germany) or Intralipid-10% (KabiVitrum, Clayton, NC) were made with a single integrating sphere. The physical properties (composition and particle size) of Intralipid are discussed in Reference 5. Collimated transmission measurements of these suspensions were made with a narrow field of view radiometer. These measurements and the properties of the sphere were used with the inverse adding-doubling (IAD) algorithm[16] to determine the optical properties of each suspension. This method repeatedly solves the radiative transport equation until the solution and the measured values of reflection and transmission are the same. All measurements were performed with a Nd:YAG laser (Holobeam) operating at the 1064-nm wavelength. The power level used was a nominal 300 mW and the $1/e^2$ beam diameter was 2 mm. The laser power was stable to within $\pm 10\%$. The suspensions were contained in a 50.8-mm diameter cell with a 5-mm path length. This cell-to-beam diameter was chosen to reduce the possibility of overestimating the absorption.[17] The cell windows were made of borosilica crown (BK-7) glass. The integrating sphere (Labsphere) had a diameter of 508 mm with an exit port diameter of 127 mm. The sphere's rotational axis was centered on the laser beam with the sphere mounted on a thrust bearing. The sphere could be rotated 180 degrees so that the sample port could be used to measure either the diffuse reflection or diffuse transmission. The collimated transmission was measured with an attachment to the exit port of the sphere. This allowed the radiometer to be placed 813 mm from the sample that was located at the entrance port of the sphere. The attachment had internal apertures of 3 mm diameter to stop the introduction of diffuse light to the collimated signal. This also provided the detector with an acceptance angle of 1.8 mrad. A schematic of the sphere measurement system is shown in Figure 1. The sphere measurements were corrected for spectral reflectance with a calibrated reflectance plate from Labsphere. The sphere and collimated transmission measurements were made with the Photodyne Model 66 XL radiometer.

To serve as a control for the integrating sphere measurements and the IAD program calculations, the optical properties of two polystyrene sphere (0.804-μm diameter) suspensions were measured. The results of these measurements were compared with those obtained by calculations based on Mie theory.[18]

The procedure and Mie theory equations that were used to determine the optical properties of the polystyrene sphere suspensions are as follows. The actual Mie calculations were performed using the algorithms of David Hahn, Sandia National Laboratories, Livermore, CA. The number density of the monodisperse suspensions of polystrene spheres was determined by measuring the collimated transmission of an HeNe laser beam (633 nm) that passed through the suspension, and calculating the extinction cross-section for the spheres. The following equations were used.

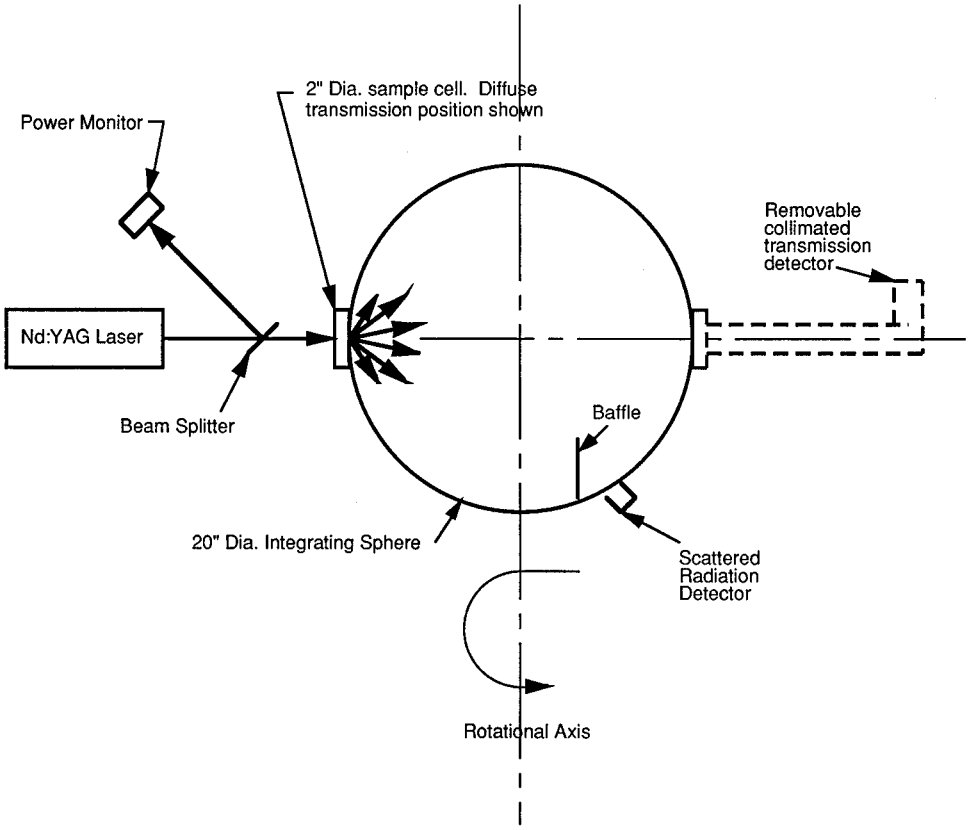

Fig. 1 Schematic illustration of the optical apparatus used to measure the phantom's diffuse reflection and transmission, and collimated transmission.

$$\tau = I_\tau / I_0 = \exp(-N \cdot C_{\text{ext}} \cdot L), \tag{1}$$

where

$$C_{\text{ext}} = C_{\text{scat}} + C_{\text{abs}}, \tag{2}$$

τ=collimated transmission, N=particle number density (particles/cm^3), C_{abs}=absorption cross-section (cm^2)=0.0 for polystyrene, C_{scat}=scattering cross-section (cm^2), C_{ext}=extinction cross-section (cm^2), L=optical path length (cm), and I_τ / I_0=collimated transmission ratio.

From Mie scattering theory for a single particle, the scattering cross-section can be determined from the following equation.[19]

$$C_{\text{scat}} = [\lambda^2/(2 \cdot \pi \cdot n_0^2)] \cdot \sum_{n=0}^{\infty} (2n+1) \cdot (|a_n|^2 + |b_n|^2), \tag{3}$$

where

$$a_n = \frac{\Psi_n(\alpha)\Psi_n'(m\alpha) - m\Psi_n(m\alpha)\Psi_n'(\alpha)}{\xi(\alpha)\Psi_n'(m\alpha) - m\Psi_n(m\alpha)\xi_n'(\alpha)}$$

$$b_n = \frac{m\Psi_n'(m\alpha)\Psi_n(\alpha) - \Psi_n(m\alpha)\Psi_n'(\alpha)}{m\Psi_n'(m\alpha)\xi_n(\alpha) - \Psi_n(m\alpha)\xi_n'(\alpha)}$$

$$m = \frac{\text{sphere index}}{\text{medium index}} = \frac{n}{n_0} = \frac{1.59}{1.33}$$

$$\alpha = \frac{2\pi a n_0}{\lambda},$$

a=radius of polystyrene sphere (cm), λ=laser wavelength in air (cm), and Ψ_n, ξ_n, Ψ_n', ξ_n' =Ricatti-Bessel functions of the first or second kind.

Using Eqs. (1) and (3) and performing the transmission measurement, the suspension's scattering coefficient at 633 nm could be determined from

$$N \cdot C_{\text{ext}} = \sigma_s = \frac{-1}{L} \ln(\tau), \tag{4}$$

where σ_s=scattering coefficient (cm^{-1}). Using Eqs. (3) and (4) allows the calculation of the particle number density (N). This value is independent of wavelength. Using this value for N and recalculating Eq. (3) at 1064 nm allows for the determination of the scattering coefficient of the suspension at

1064 nm. For the polystyrene spheres, the index of refraction was assumed to be the same at 1064 nm as it is in the visible ($\bar{n}$=1.59+0.00i).

The anisotropy or g [referred to as the asymmetry factor ($\overline{\cos\theta}$) in Ref. 19] was calculated from the following equation:

$$g=\overline{\cos\theta}=\frac{\lambda^2}{\pi n_0^2 C_{\text{scat}}}\left\{\sum_{n=1}^{\infty}\frac{2n+1}{n(n+1)}\,\text{Re}(a_n b_n^*)+\sum_{n=1}^{\infty}\frac{n(n+2)}{n+1}\,\text{Re}(a_n a_{n+1}^*+b_n b_{n+1}^*)\right\}, \tag{5}$$

where an asterisk indicates that the complex conjugate is to be taken.

Dilutions of either India ink or Intralipid-10% were made with deionized water. The ink concentrations ranged from 0.05 to 0.5% by volume (volume of ink divided by the sum of the volume of ink and water). The Intralipid concentrations ranged from 1.0 to 4.0% by volume. Each suspension was placed into the cell and five readings of collimated and diffuse transmission and diffuse reflection were made. These values were averaged. This process was repeated five times for each concentration. Measurement computations were performed in a manner similar to those outlined by Prahl[16] and Pickering.[20] Average values and standard deviations for these data were determined. A linear curve fit was applied to all the Intralipid and India ink data. The zero concentration intercept value of the fitted equation gives an indication of how well the data are represented, while the slope value can be compared with historical values.[5]

After the optical properties of the ink and the Intralipid were determined, two optical phantoms were made, one with ink and Intralipid and one with Intralipid only. The design optical properties of the first phantom were μ_a = 0.37 cm^{-1}, and μ_s = 8.2 cm^{-1}, while those of the second phantom were assumed to be μ_a = 0.00 cm^{-1} and μ_s = 8.2 cm^{-1}. These optical properties are similar to those reported in Reference 21 for canine prostate. The optical properties of these phantoms were then measured in a manner similar to that for the diluted Intralipid or ink suspensions. The phantoms were constructed based upon the Intralipid scattering data (μ_s/%), and the India ink absorption data (μ_a/%). The slope of these lines determined the amount of ink and Intralipid to mix with 200 ml of deionized water to obtain the design optical properties. These phantoms were constructed under the assumption that neither Intralipid nor water absorbed light, and India ink didn't scatter light. This was done in order to simplify their construction as well as duplicate current first-order construction procedures.

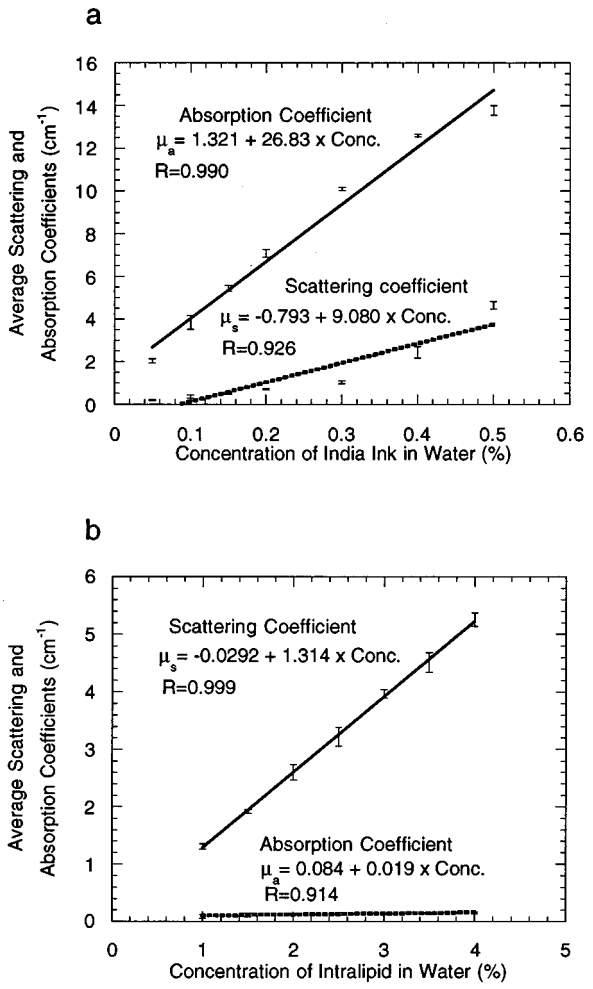

Fig. 2 The absorption and scattering coefficients at 1064 nm for varying concentrations of water suspensions of (a) India ink and (b) Intralipid-10%.

3 RESULTS

The two 804-nm diameter polystyrene sphere and water suspensions produced a Mie theory-predicted scattering coefficient of 2.23 cm^{-1} and 2.96 cm^{-1}. The Mie theory calculation of the anisotropy for these solutions was 0.807. The average of four trial measurements for the first solution gave μ_a=0.28±0.02 cm^{-1}, μ_s=1.99±0.12 cm^{-1}, and g=0.775±0.04. The average of two trials for the second solution gave μ_a=0.25±0.01 cm^{-1}, μ_s=3.15 ±0.01 cm^{-1}, and g=0.811±0.004. These absorption coefficients have not been corrected for water absorption.

The optical properties (μ_a, μ_s, g) resulting from the IAD calculations for different concentrations of India ink and Intralipid-10% are shown in Figures 2 and 3. (In all figures the error bar length is two standard deviations, and R is the linear correlation coefficient.) Figure 2 shows the average absorption and scattering coefficients as a function of India ink or Intralipid concentrations. The average optical

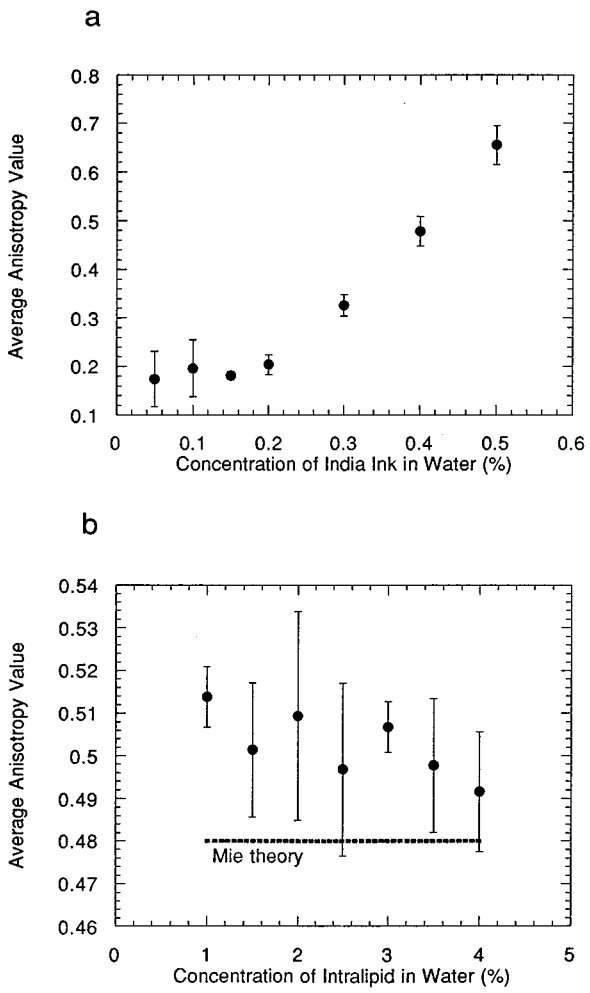

Fig. 3 The anisotropy at 1064 nm for varying concentrations of water suspensions of (a) India ink and (b) Intralipid-10%. The Mie theory value is taken from Ref. 5.

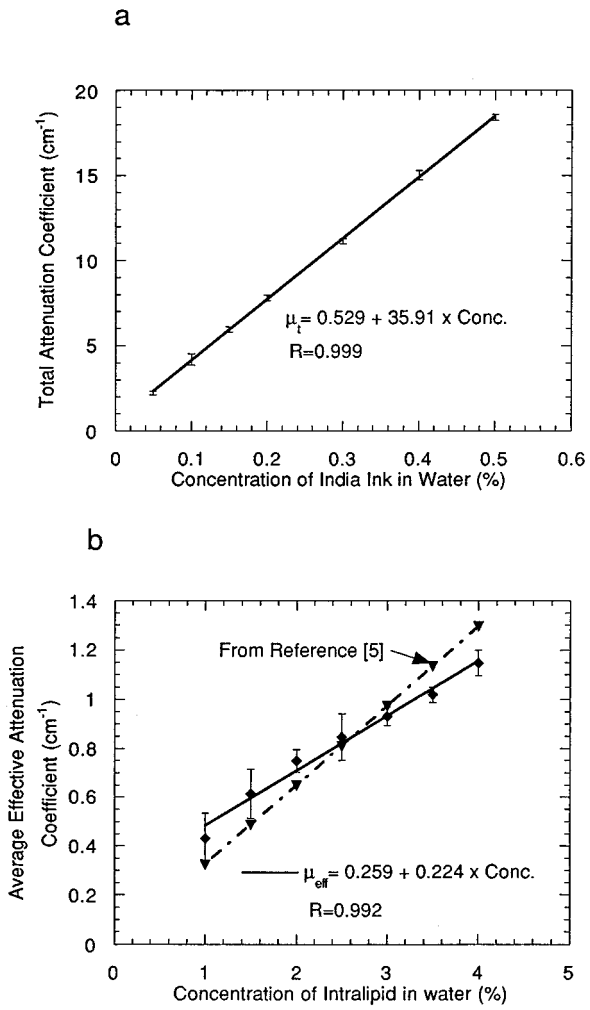

Fig. 4 The attenuation coefficients at 1064 nm for varying concentrations of water suspensions of (a) India ink and (b) Intralipid-10%. The total attenuation coefficient is plotted for the India ink's highly absorbing suspensions. The effective attenuation coefficient is plotted for Intralipid's highly scattering suspensions. The dotted plot in (b) is taken from data in Ref. 5.

properties from all the data are shown in Table 1. (Note: The absorption per concentration value of Intralipid has been corrected for water absorption.) Figure 3 shows the average anisotropy factor as a function of India ink or Intralipid concentration.

Since absorption dominates the light distribution in India ink, the total average attenuation coefficient ($\mu_t = \mu_a + \mu_s$) is shown in Figure 4(a). However, since scattering dominates the light distribution in Intralipid,[22] the effective attenuation coefficients were determined from the Intralipid data presented in Figures 2 and 3. These data are shown in Figure 4(b).

Table 1 Average optical property concentrations of India ink, Intralipid, and water at 1064 nm. The water absorption is taken from Ref. 23. The absorption results of Intralipid are corrected for water absorption. These data are the average values of all data points.

Scattering media	μ_s/% (cm^{-1}/%)	μ_a/% (cm^{-1}/%)	g
India ink	4.64±2.07	35.99±4.28	0.30±0.18
Intralipid	1.30±0.047	0.054±0.02	0.50±0.02
Water	—	0.0018	—

The ink and Intralipid phantoms were constructed based upon the fitted straight-line slopes of 26.83 cm^{-1}/% and 1.31 cm^{-1}/% for ink and Intralipid respectively. For a phantom with μ_a=0.32 cm^{-1} and μ_s = 8.82 cm^{-1}, these slopes indicated a phantom composed of 0.01% ink, 6.69% Intralipid, and 93.30% water. The phantom without any ink (assuming that μ_a = 0.00 cm^{-1}) contained 6.70% Intralipid. A comparison of the predicted, measured, and calculated optical properties of the two phantoms is shown in Table 2.

Table 2 Predicted and measured optical properties of phantoms. The predicted values for phantoms 1 and 2 assume that Intralipid and water do not absorb and that ink does not scatter 1064-nm light. The calculated values were determined from the concentration values found in Table 1.

Phantoms	μ_s(cm^{-1})	μ_a(cm^{-1})	g
Phantom 1 (IL and ink)			
Predicted	8.82	0.32	0.48 [5]
Measured	9.69±0.22	0.76±0.01	0.56±0.00
Calculated	8.75	0.89	0.50
Phantom 2 (IL only)			
Predicted	8.82	0.00	0.48
Measured	8.84±0.03	0.33±0.01	0.51±0.00
Calculated	8.70	0.53	0.50

4 DISCUSSION

For the polystyrene sphere suspensions, the agreement between the Mie calculations and the integrating sphere measurements and IAD calculations for the scattering coefficient was good (2.23 versus 1.99 and 2.96 versus 3.15). For anisotropy, the agreement was also good (0.807 versus 0.775 and 0.811). These solutions had an average albedo, a ($a = \mu_s / \mu_t$) of 0.88±0.03 and 0.93±0.00 and optical depths, b ($b = (\mu_a + \mu_s)\cdot$cell solution thickness) of 1.13±0.03 and 1.70±0.00. These values are within the recommended ranges for highest accuracy when using the IAD algorithm.[16] These recommended ranges are albedos of 0.4 to 0.95 and optical depths of 1 to 10.

While the ink's albedo (0.25 to 0.08) was always outside the IAD's recommended range of 0.4 to 0.95, the linearity of the absorption coefficient with concentration was very good [Figure 2(a)]. The scattering coefficient for Intralipid is also linear with concentration [Figure 2(b)]. The value for the slope of this fitted line, 1.31 cm^{-1}/%, is the same as the value presented in Reference 5. The zero concentration intercept values for the straight-line equations are shown in Figure 2. Ideal zero concentration values would be equal to the absorption or scattering coefficient for water (0.182, or 0.118 cm^{-1} for absorption from References 23 and 24, and an assumed scattering value of 0.00 cm^{-1}). The Intralipid's zero concentration intercept values (0.08 and −0.03) are closest to those of water, while ink's values are more divergent (−0.8 and 1.3).

The anisotropy of the ink and Intralipid solutions should not change with concentration. This is the case for the Intralipid data, but fails for the ink data, as shown in Figure 3. Two reasons may contribute to the nonlinear behavior of the ink solutions's anisotropy.

The first reason is that the particle size distribution of the ink solution changes with higher concentrations. Ink is made up of a collection of small (0.1 μm) and large particles (1.0 μm).[6] The small particles have a low anisotropy value while the larger ones have a much higher value. As the concentration of the larger particles increases, the albedo of the ink also increases. Figure 2(a) shows that the ink's scattering coefficient increases with increasing concentration. At the higher concentrations of ink (0.3, 0.4, and 0.5), the ink's larger particles may be strongly influencing the solution's albedo and anisotropy. At the higher concentrations there may also be a tendency for the ink particles to coalesce. A surfactant is commonly added to a solution of rhodamine dye (powder form) and water to prevent particle coalescence. Adding a similar surfactant to ink solutions may also play a role in reducing any ink particle coalescence.

The second reason for this nonlinear anisotropy behavior may be computational. The lack of sufficient diffuse transmission signal strength for ink concentrations greater than 0.2% may not allow the IAD algorithm to arrive at an accurate solution for the anisotropy value.

The average ink albedo was 0.12±0.06. This is lower than the previously measured ink albedo for visible light (>0.3).[6] Thus, the scattering of India ink is lower at 1064 nm than that reported at 594 nm. This seems reasonable since the scattering coefficient is proportional to the inverse of the wavelength raised to a power between 1 and 2 for tissue.[25] For India ink, with a nearly linear absorption coefficient and relatively small scattering coefficient [Figure 2(a)], the total attenuation coefficient follows the absorption coefficient's linearity [Figure 4(a)]. The value of the fitted slope, 35.91 cm^{-1}/%, is very close to the average optical property concentration value of 35.99 cm^{-1}/% (Table 1). The scattering coefficient of the ink increases as the concentration of ink increases (possibly due to more large ink particles), but this does not seem to affect the linearity of the total attenuation coefficient.

The effective attenuation coefficients for Intralipid suspensions show an almost linear response with concentration [Figure 4(b)]. This is similar to results obtained by Driver et al. for 630-nm laser light.[15] Using different methodology, they showed a loss in linearity of Intralipid's effective attenuation coefficient for low concentrations. They attributed this loss to the absorption of water at the low concentrations. The effective attenuation coefficients plotted in Figure 4(b) have been corrected for water absorption. The effective attenuation coefficient of Intralipid suspensions can also be calculated from the values for Intralipid's optical properties at 1064 nm that are reported in Reference 5. These are plotted and also shown in Figure 4(b). Since the scattering concentration slopes are identical, the difference in the two curves can be attrib-

uted to the difference in their absorption concentration slopes: 0.054 and 0.048 $cm^{-1}/\%$.

If the values listed in Table 1 are used to determine the optical properties of the first phantom by including the ink scattering and the Intralipid and water absorption, then the calculated optical properties become $\mu_a = 0.89\ cm^{-1}$ and $\mu_s = 8.75\ cm^{-1}$. Comparing these calculated values with the measured values in Table 2 shows that the measured absorption ($0.76\ cm^{-1}$) is lower and the scattering coefficient ($9.69\ cm^{-1}$) is higher. These calculated values depend upon the average of all the data points, and may be influenced by the lack of ink anisotropy linearity and an apparent discrepancy for the value of the water absorption coefficient at 1064 nm. Two references[23,24] give differing values, $0.182\ cm^{-1}$ and $0.118\ cm^{-1}$, for a water absorption coefficient at 1064 nm.

By knowing the dependence of scattering and absorption of the ink and Intralipid, a phantom with predicted optical properties can be constructed. However, the constructed phantom's final optical properties should be measured for an accurate determination of the phantom's optical properties.

5 CONCLUSIONS

The optical properties of Intralipid and India ink suspensions at 1064 nm were determined by making three optical measurements and using the IAD algorithm along with the optical constants of the integrating sphere. Both the absorption of Intralipid suspensions and the scattering of India ink suspensions are small at the Nd:YAG laser wavelength of 1064 nm. When phantoms with high absorption (low albedo) are used, the IAD algorithm may fail to accurately predict the phantom's anisotropy.

NOTES

The mention of commercial products or their use in connection with material reported here is not to be construed as either an actual or implied endorsement of such products by the U.S. Food and Drug Administration.

The actual Mie calculations were performed using the algorithms of David Hahn, Sandia National Laboratories, Livermore, CA.

REFERENCES

1. C. J. M. Moes, M. J. C. Van Gemert, W. M. Star, J. P. A. Marijnissen, and S. A. Prahl, "Measurements and calculations of the energy fluence rate in a scattering and absorbing phantom at 633 nm," *Appl. Opt.* **28**, 2292–2296 (1989).
2. W. M. Star, J. P. A. Marijnissen, and M. J. C. Van Gemert, "Light dosimetry in optical phantoms and in tissues. 1: Multiple flux and transport theory," *Phys. Med. Biol.* **33**, 437–454 (1988).
3. A. J. Durkin, S. Jaikumar, and R. Richards-Kortum, "Optically dilute, absorbing, and turbid phantoms for fluorescence spectroscopy of homogeneous and inhomogeneous samples," *Appl. Spectro.* **47**, 2114–2121 (1993).
4. C. F. Bohren and D. R. Huffman, *Absorption and Scattering of Light by Small Particles,* Wiley, New York (1983).
5. H. J. Van Staveren, C. J. M. Moes, J. Van Marle, S. A. Prahl, and M. J. C. Van Gemert, "Light scattering in Intralipid-10% in the wavelength range of 400–1100 nm," *Appl. Opt.* **30**, 4507–4514 (1991).
6. S. J. Madsen, M. S. Patterson, and B. C. Wilson, "The use of India ink as an optical absorber in tissue-simulating phantoms," *Phys. Med. Biol.* **37**, 985–993 (1992).
7. W. Cheong, S. A. Prahl, and A. J. Welch, "A review of the optical properties of biological tissues," *J. Quan. Elec.* **26**, 2166–2185 (1990).
8. S. N. Joffe and Y. Oguro, Eds., *Advances in Nd:YAG Laser Surgery,* Springer-Verlag, New York (1988).
9. J. N. Kabalin, "Transurethral laser prostatectomy," *Infect. Urology* May/June, 71–84 (1994).
10. A. C. Steger, "Interstitial laser hyperthermia for the treatment of hepatic and pancreatic tumors," *Photochem. Photobio.* **53**, 837–844 (1991).
11. K. Rothenberger, J. Pensel, A. Hofstetter, E. Keiditsch, and F. Frank, "Transurethral laser coagulation for treatment of urinary bladder tumors," *Lasers Surg. Med.* **2**, 255–260 (1983).
12. M. Panjehpour, B. F. Overholt, D. L. Frazier, and E. R. Klebanow, "Nd:YAG laser-induced hyperthermia treatment of spontaneously occurring veterinary head and neck tumors," *Lasers Surg. Med.* **11**, 351–355 (1991).
13. A. El-Ouahabi, C. R. G. Guttmann, S. G. Hushek, A. R. Bleier, K. Dashner, P. Dikkes, P. M. Black, and F. A. Jolesz, "MRI guided interstitial laser therapy in a rat malignant glioma model," *Lasers Surg. Med.* **13**, 503–510 (1993).
14. V. Allen and A. L. McKenzie, "The modified diffusion dipole model," *Phys. Med. Biol.* **36**, 1621–1638 (1991).
15. I. Driver, J. W. Feather, P. R. King, and J. B. Dawson, "The optical properties of aqueous suspensions of intralipid, a fat emulsion," *Phys. Med. Biol.* **34**, 1927–1930 (1989).
16. S. A. Prahl, M. J. C. Van Gemert, and A. J. Welch, "Determining the optical properties of turbid media by using the adding-doubling method," *Appl. Opt.* **32**, 559–568 (1993).
17. J. H. Torres, A. J. Welch, I. Cilesiz, and M. Motamedi, "Tissue optical propety measurements: overestimation of absorption coefficient with spectrophotometric techniques," *Lasers Surg. Med.* **14**, 249–257 (1994).
18. J. V. Dave, "FORTRAN subroutine DBMIE," IBM Palo Alto Scientific Center Report No. 320-3237 (May 1968).
19. M. Kerker, *The Scattering of Light and Other Electromagnetic Radiation,* Academic Press, New York (1969).
20. J. W. Pickering, S. A. Prahl, N. Van Wieringen, J. F. Beek, H. J. C. M. Sterenborg, and M. J. C. Van Gemert, "Double-integrating-sphere system for measuring the optical properties of tissue," *Appl. Opt.* **32**, 399–410 (1993).
21. B. Anvari, M. Motamedi, J. Torres, R. Huang, S. Rastegar, and S. L. Jacques, "Optical properties of native and coagulated canine prostate," *Lasers Surg. Med.* **Supp. 5** (1993).
22. B. C. Wilson and S. L. Jacques, "Optical reflectance and transmittance of tissue: principles and applications," *J. Quan. Elec.* **26**, 2186–2189 (1990).
23. G. H. Suits, "Natural Sources," in *The Infrared Handbook,* W. L. Wolfe and G. J. Zissis, Eds., Chapter 3, pp. 3–110, ERIM, Ann Arbor, MI (1978).
24. G. M. Hale and M. R. Querry, "Optical constants of water in the 200 nm to 200 μm wavelength region," *Appl. Opt.* **12**, 555–563 (1973).
25. M. J. C. Van Gemert, A. J. Welch, S. L. Jacques, W. F. Cheong, and W. M. Star, "Light distribution optical properties, and cardiovascular tissues," in *Laser Angioplasty,* G. Abela, Ed., Chapter 8, pp. 93–110, Wiley, New York (1991).